Migratory monocytes and granulocytes are major lymphatic carriers of *Salmonella* from tissue to draining lymph node

Michel Bonneau,* Mathieu Epardaud,† Fabrice Payot,† Violeta Niborski,† Maria-Isabel Thoulouze,†,‡ Florence Bernex,§ Bernard Charley,† Sabine Riffault,† Laurence A. Guilloteau,¶ and Isabelle Schwartz-Cornil†,[1]

**Centre de Recherche en Imagerie Interventionnelle, Jouy-en-Josas, France; †Virologie et Immunologie Moléculaires UR892 INRA, Jouy-en-Josas, France; ‡Institut Pasteur, Paris, France; §UMR 955 INRA/ENVA de Génétique Moléculaire et Cellulaire and Service d'Anatomie Pathologique, Ecole Nationale Vétérinaire d'Alfort, Maisons-Alfort, France; and ¶Pathologie Infectieuse et Immunologie INRA, Nouzilly, France*

Abstract: Dendritic cells (DC) are recognized as sentinels, which capture antigens in tissue and migrate to the lymph node, where they initiate immune responses. However, when a vaccine strain of green fluorescent protein-expressing *Salmonella abortusovis* (SAO) was inoculated into sheep oral mucosa, it induced accumulation of myeloid non-DC in the subcapsular sinus and paracortex of the draining lymph node, and SAO was mainly found associated with these cells (granulocytes and macrophages) but rarely with DC. To analyze how bacteria reached lymph nodes, we used cervical pseudo-afferent lymph duct catheterization. We showed that *Salmonella* administered in the oral mucosa were traveling free in lymph or associated with cells, largely with lymph monocytes and granulocytes but less with DC. SAO also induced a strong influx of these phagocytic cells in afferent lymph. Migrating DC presented a semi-mature phenotype, and SAO administration did not alter their expression of major histocompatibility complex type 2 and coactivation molecules. Compared with blood counterparts, lymph monocytes expressed lower levels of CD40, and granulocytes expressed higher levels of CD80. The data suggest that immunity to bacteria may result from the complex interplay between a mixture of phagocytic cell types, which transport antigens and are massively recruited via lymph to decisional lymph nodes. *J. Leukoc. Biol.* 79: 268–276; 2006.

Key Words: *dendritic cells · macrophages · cell trafficking · sheep*

INTRODUCTION

It is commonly accepted that antigens are captured in nonlymphoid tissues by dendritic cells (DC), which subsequently traffic via afferent lymphatics to the T cell area of the draining lymph node to initiate immune response [1]. However, this linear view has been challenged by several reports, indicating that antigens can reach lymph nodes via ways other than via DC. It is notable that a subcutaneously (s.c.) injected soluble antigen was shown to reach lymph nodes in two successive waves, which induce functionally distinct T cell responses: First, the soluble antigen travels freely in lymph and is picked up by resident lymph node macrophages and DC; later, the antigen gains lymph nodes within migrating, dermal DC [2]. Regarding particles, intradermally injected latex microspheres were found phagocytosed locally in tissue by inflammatory monocytes, among which 25% migrated to the lymph node, where they acquired some DC markers [3]. It is interesting that when *Salmonella* were coinjected with latex beads, bead transport to lymph nodes and monocyte conversion to DC were reduced potently [4]. However, the way *Salmonella* antigens themselves reach the lymph node to elicit an immune response was not assessed [4]. Finally, it was shown that translocated latex particles from the lung migrate to the tracheobronchial node associated with neutrophils and alveolar macrophages [5, 6] and that bacillus Calmette-Guerin (BCG) shuttles from tissue to lymph nodes via neutrophils [7]. Thus, antigens may reach lymph nodes via several modalities, which are generally difficult to comprehend using available animal models and may depend on the administration route and on the nature of the antigen.

To analyze *Salmonella* transportation from tissue to lymph node, we used a pseudo-afferent (PA) cervical lymph collection in a sheep model, which we have developed recently to monitor lymph traffic from facial mucosae [8]. PA lymph duct catheterizations have been performed previously in several instances to probe cell migration from drained tissues in different animal species [9, 10], but they have been barely used to analyze antigen transport [11]. An advantage of sheep over rat PA lymph models is that sheep can live with a permanent lymph catheter for weeks. In our cervical PA lymph model, preliminary experiments showed that latex beads deposited on oral mucosae could be tracked in lymph and were found migrating freely or associated with cells. To use this lymphatic model for analyzing microbial transport, *Salmonella abortusovis* (SAO) Rv-6 strain was chosen as a sheep-adapted, attenuated vaccine

[1] Correspondence: VIM UR892 INRA, Domaine de Vilvert, 78352 Jouy-en-Josas Cedex, France. E-mail: isabelle.schwartz@jouy.inra.fr

Received June 1, 2005; accepted October 19, 2005; doi: 10.1189/jlb.0605288

strain [12]. We found that green fluorescent protein (GFP)-expressing SAO (GFP-SAO) administration in the oral mucosa rapidly triggered accumulation of $CD11b^{pos}$ non-DC in the subcapsular and paracortical zones of the submaxillary node and was found mainly in these cells and rarely in DC. By probing PA lymph, we found that SAO transportation occurred via several modalities, i.e., free in lymph or associated with lymph monocytes and granulocytes but more rarely with DC. Establishment of immune responses will likely result from the interplay between these antigen-transporting cell types, which migrate with the antigen from the invaded tissue toward the inductive lymph node.

MATERIALS AND METHODS

Animals and surgical procedures

Prealpe female sheep (2–4 years old) were raised and housed in the Unité Commune d'Expérimentation Animale (Jouy-en-Josas, France). PA cervical lymph duct cannulations were performed as described [8]. Three cervical cannulations out of height successfully led to lymph flowing for more than 10 days and could be used for the subsequent experiments, as sheep could thus be manipulated away from possible effects post-surgery. All animal experiments were carried out under the authority of a license issued by the Direction des Services Vétérinaires (Versailles, France; accreditation numbers 78–20, 78–15, and A78730).

Lymph and blood cells

PA lymph was collected in sterile flasks with 500 IU heparin, spun down at 700 g, and the cell pellet was suspended in RPMI plus 4% horse serum (HS). Peripheral blood leukocytes (PBL) were obtained from buffy coats on citrate. Red blood cells were lysed with NH_4Cl. Peripheral blood mononuclear cells (PBMC) were obtained by Percoll gradient purification as described previously [13].

SAO injections

GFP-SAO live vaccine Rv-6 strain was used for the injections. The attenuated SAO Rv-6 was obtained as a streptomycin-sensitive revertant from a streptomycin-resistant strain derived from the original 15/5 isolate [14], which was derived from a ewe placenta after abortion. Attenuated SAO Rv-6 disseminates only to the draining lymph node, whereas the virulent 15/5 SAO disseminates widely to the spleen [15]. Two types of GFP-SAO were prepared by electrotransformation with two different plasmids encoding GFP. One plasmid was the pFPV 25.1 [16], and the other one was the pBRD940 containing the gene for GFP under the control of the *nirB* promoter (kindly provided by Susan Paulin, Institute for Animal Health, Compton, UK) [17]. For lymph collection, a mixture of the two GFP-SAO transformants [5×10^8 colony-forming units (CFU) each] was injected as 50 μl spots in the oral mucosae (tongue, cheeks, lips) with a 30-gauge needle in endotoxin-free 0.9% NaCl in three anesthetized sheep-bearing canula. Lymph cells were collected before and after SAO administration during specified collection periods. For submaxillary lymph node analysis, the GFP-SAO mixture (5×10^8 CFU each) was injected under 50 μl spots in the left oral mucosa, and the left submaxillary lymph node was collected at slaughtering 3, 6, and 20 h post-inoculation. The contralateral lymph node was harvested at the same time. Half of the node was minced in RPMI plus 2% fetal calf serum to harvest lymph node cells. Three specimens per node were frozen in optical cutting temperature compound tissue-mounting gel (Baxter, Deerfield, IL) and cold isopentane bath.

Antibodies

Monoclonal antibodies (mAb) directed against sheep molecules are described in **Table 1**. The polyclonal anti-human CD3 (Dako, Carpinteria, CA) cross-reacts with sheep cells [18, 19]. IgG1 isotype control is clone KP-53, directed against the human κ chain (Sigma-Aldrich, St. Louis, MO), and IgG2a isotype control is clone PK136, directed against mouse NK-1.1 (Becton Dickinson, Mountain View, CA).

TABLE 1. Anti-Sheep Molecule Murine mAb

Molecule	mAb	Isotype	Origin
CD1b	TH97A	IgG2a	VMRD[a]
CD4	ST4	IgG1	W. Hein[b]
CD11b	MM12A	IgG1	VMRD
CD11b	ILA130	IgG2a	J. Naessens[b]
CD11c	OM1	IgG1	M. Pépin[b]
CD14	TUK4	IgG2a	Caltag[c]
CD14	CAM36	IgG1	VMRD
CD40	ILA156	IgG1	J. Naessens
CD62L	DU1–29	IgG1	VMRD
CD80	ILA159	IgG1	J. Naessens
CD86	ILA190	IgG1	J. Naessens
DC-LAMP	104.G4	IgG1	Beckman[d]
MHC 2	CAT82A	IgG1	VMRD
MHC 2	TH14B	IgG2a	VMRD

[a] VMRD, Veterinary Medical Research and Development (Pullman, WA). [b] The mAb were provided by academic laboratories [Jan Naessens (ILRI, Kenyia), Michel Pépin (AfSSA, France), and Wayne Hein (AgResearch, New Zealand)]. [c] Caltag Laboratories (Burlingame, CA). [d] Beckman-Coulter Inc. (Fullerton, CA). IgG, Immunoglobulin G; DC-LAMP, DC-lysosome-associated membrane protein; MHC 2, major histocompatibility complex type 2.

Lymph node section staining

Lymph node cryosections (4 μm) were prepared on charged slides and fixed in cold acetone. CD3/CD11b double-labeling was done with a polyclonal rabbit anti-CD3 (2 μg/ml), revealed by a fluorescein isothiocyanate (FITC) goat anti-rabbit IgG (Jackson ImmunoResearch, West Grove, PA), and with the anti-CD11b ILA130 mAb, revealed by an Alexa-fluor 594-conjugated goat anti-mouse (GAM) IgG (Molecular Probes, Junction City, OR). DC-LAMP/CD11b double-staining was performed with the 104.G4 mAb, revealed by a FITC-GAM IgG1 (Caltag Laboratories), and ILA130, revealed by a tetramethylrhodamine isothiocyanate (TRITC)-conjugated Fab′2 GAM IgG2a (Jackson ImmunoResearch). The cell nuclei were stained with 4′,6-diamidino-2-phenylindole (DAPI) for 5 min, and the slides were mounted in Vectashield (Vector Laboratories, Burlingame, CA). The slides were observed using a classical fluorescence microscope (Leica) or with a confocal microscope [Leica TCS Spectral (SP1)], equipped with a DMR-inverted microscope and a 63× objective with a numerical aperture of 1.4. A krypton-argon mixed-gas laser was used to generate two bands: 488 nm for FITC and 568 nm for TRITC.

Immunophenotyping analysis by flow cytometry

Lymph node cells, lymph cells, PBL, and PBMC were incubated in fluorescein-activated cell sorter (FACS) medium (RPMI 1640 containing 4% HS and 0.02% sodium azide) for 15 min on ice. Cells (>95% viability, 2×10^6) were reacted with primary mAb in FACS medium for 30 min at 4°C. After two washes, they were incubated further with a 1:200 dilution of FITC-, phycoerythrin (PE)-, or tricolor-GAM antibodies, directed to light and heavy G chains or to specific isotypes (Caltag Laboratories) for 30 min at 4°C. Cells were then washed twice in FACS medium. Irrelevant murine IgG1 and IgG2a were used as negative controls.

Labeled cells were suspended in 300 μl CellFix (Becton Dickinson), and cells were analyzed with a FACSCalibur™ using CELLQuest ™ software (Becton Dickinson).

Lymph cell morphology

FITC-GAM-labeled $CD1b^{pos}$, $CD14^{int}$ FSC^{lo}, and $CD14^{hi}$ FSC^{lo} cells were isolated using the sort module of a FACSCalibur, and cytospots were prepared. The slides were stained with May-Grunwald-Giemsa (MGG) or were reacted with an Alexa fluor 488-conjugated rabbit anti-FITC (25 μg/ml, Molecular Probes), fixed with 1% paraformaldehyde, and incubated in DAPI (0.25 μg/ml)

for nuclear staining. The slides were mounted in Vectashield and analyzed using transmitted light and fluorescence microscopy.

Immunocytochemistry for MHC 2 and DC-LAMP localization in lymph cells

Low-density lymph cells were prepared from freshly collected cells. They were enriched over a 1.065 density iodixanol gradient (Optiprep, Nycomed Pharma, Oslo, Norway). Cytospin preparations (2×10^5) in 100 μl RPMI were made and subsequently fixed in acetone. After extensive drying, the slides were rehydrated and incubated in RPMI containing 10% HS for 30 min. Cells were reacted with 1 μg/ml anti-MHC 2 (TH14B, IgG2a) and 2 μg/ml anti-DC-LAMP (104.G4, IgG1) in RPMI 1640 plus 10% HS for 30 min. After three washes, TH14B and 104.G4 binding were revealed by a 1:100 dilution of a TRITC-conjugated Fab′2 GAM IgG2a (Jackson ImmunoResearch) and a 1:100 dilution of a FITC-GAM IgG1 (Caltag Laboratories), respectively. The slides were washed six times, mounted in Vectashield, and observed with a confocal microscope as described above.

Mixed leukocyte reaction (MLR)

Lymph was collected for 4 h before and for a period between 20 and 24 h after injection of bacteria. Lymph cells labeled with anti CD1b (TH97A) were sorted with immunomagnetic beads [GAM IgG-specific, magnetic cell sorter (MACS), Miltenyi Biotec, Germany] and were plated in 96-well plates in X-vivo 20 medium (BioWhittaker, Walkersville, MD) at a different ratio with 10^5 allogeneic CD4 immunomagnetically purified T cells (selected with ST4 mAb followed by GAM IgG-specific, coated beads, MACS). After 96 h, the cultures were pulsed for 18 h with 1 μCi [^{3}H]-thymidine.

RESULTS

GFP-SAO are mainly associated with recruited CD11b^{pos} non-DC in subcapsular, interfollicular, and T cell zones of the draining lymph node

To assess the cellular association of GFP-SAO in lymph nodes soon after injection, bacteria were administered in the sheep oral mucosa, and preparations of lymph node cells were analyzed by flow cytometry. Twenty hours after injection, the vast majority of the GFP-SAO was associated with CD11b^{pos} cells and rarely with CD1b^{pos} cells (**Fig. 1A**). CD11b defines myelomonocytic cells in sheep (macrophages, monocytes, and granulocytes) [20] and does not stain DC [20], whereas CD1b is generally used to identify DC [8, 11]. A clear influx of CD11b^{pos} cells was observed in the draining lymph node at 20 h (Fig. 1A). The CD11b^{pos} cells from draining lymph nodes, visualized by fluorescent microscopy, included cells with nuclear morphologies of granulocytes and macrophages (DAPI staining in Fig. 1B). In lymph node sections, as early as 3 h post-administration, bacteria were frequently visible in the subcapsular zone where huge amounts of CD11b^{pos} cells accumulated (Fig. 1D compared with contralateral node Fig. 1C). Similar observations were done at 6 h (not shown). Bacteria were seen associated with CD11b^{pos} cells presenting a granulocyte or macrophage nuclear morphology (Fig. 1, H1 and H2). Confocal examination showed that bacteria were most often inside CD11b^{pos} cells (Fig. 1, H3). At a later time-point (20 h), CD11b^{pos} cells, occasionally with intact bacteria, were found infiltrating the interfollicular area and the paracortex, in contact with CD3^{pos} T cells (Fig. 1, E and I). However, intact bacteria were more difficult to find at 20 than at 3 h. This was likely a result of reduced GFP fluorescence under prolonged in vivo conditions, as CFU countings were higher at 20 h (approximately 3×10^6 CFU per lymph node) than at 3 h (10^6 CFU per lymph node). In the paracortex (T cell zone), hematoxylin staining revealed cells with morphology of macrophages and numerous granulocytes (Fig. 1G). It is notable that by 20 h, many clusters of DC-LAMP^{pos} cells and CD11b^{pos} cells were visible in the T cell zone (Fig. 1F), and intimate cell interactions were seen by confocal examination (Fig. 1J), suggesting that cooperation between DC and other myeloid non-DC occurred in inductive regions of the lymph node.

Altogether, the results indicate that SAO bacteria were initially found in the subcapsular area, mainly carried by non-DC myeloid cells with features of granulocytes and macrophages. Later, SAO were detected in the paracortex associated with non-DC myeloid cells, suggesting that these cells could transport bacteria down to inductive areas of the node. The early accumulation of inflammatory cells loaded with bacteria in the subcapsular area suggests the hypothesis that these cells may exit from tissue with bacteria and transport them via lymph ducts.

SAO induces an influx of phagocytes in afferent lymph and is transported free or associated with granulocytes, monocytes, and rarely to DC

To address the possible contribution of monocytes and/or granulocytes in shuttling *Salmonella* from tissue to lymph nodes, we used an approach based on PA lymph duct catheterization. Three sheep, cannulated successfully for periods extending over 10 days post-surgery, were used to get minimal inflammation from the surgical procedure. We then needed to be able to track DC, monocytes, and granulocytes in lymph. CD1b has been identified previously as a reliable marker to characterize migrating DC [8, 11]. CD11b similarly stains monocytes and granulocytes (see Figs. 1 and 5), so it cannot be used to distinguish monocytes from granulocytes. It is interesting that in human, CD14 has been used to discriminate between monocytes (CD14^{hi}) and granulocytes (CD14^{int}) [21, 22], and CD14 has been described previously to react with sheep blood granulocytes and monocytes [18]. CD14 expression was thus evaluated for its capacity to distinguish granulocytes and monocytes in sheep lymph (**Fig. 2**). CD14^{int} and CD14^{hi} were gated on lymph cells excluded of the large cells, which correspond to DC (see Fig. 4). When sorted, the CD14^{int} cells included over 90% granulocytes, as attested by their poly-segmented nuclear morphology in MGG and DAPI staining (Fig. 2, R1). The CD14^{int} cells also presented a low FSC/high SSC profile (Fig. 2, R1). Similarly, the CD14^{hi} cells were sorted and found to display a monocyte morphology revealed by MGG and rod-shaped DAPI nuclear staining (Fig. 2, R2). CD14^{hi} cells were associated with a low FSC/low SSC profile (Fig. 2, R2).

Administration of GFP-SAO induced a rapid mobilization of CD1b^{pos} and CD14^{pos} cells in lymph (**Table 2**). During the first 90 min post-SAO injection in three sheep, we could evaluate that SAO augmented the output of DC by 2.2-fold (±0.04), of granulocytes by 4.8-fold (±1.4), and of monocytes by 6.3-fold (±4). Conversely, T and B cell lymph output was not affected, and overall, the total lymph cell rate was not changed and was similar between sheep (approximately 5×10^6/ml, data not shown). Regarding bacterial transport during the same period, most GFP-SAO were found free in lymph

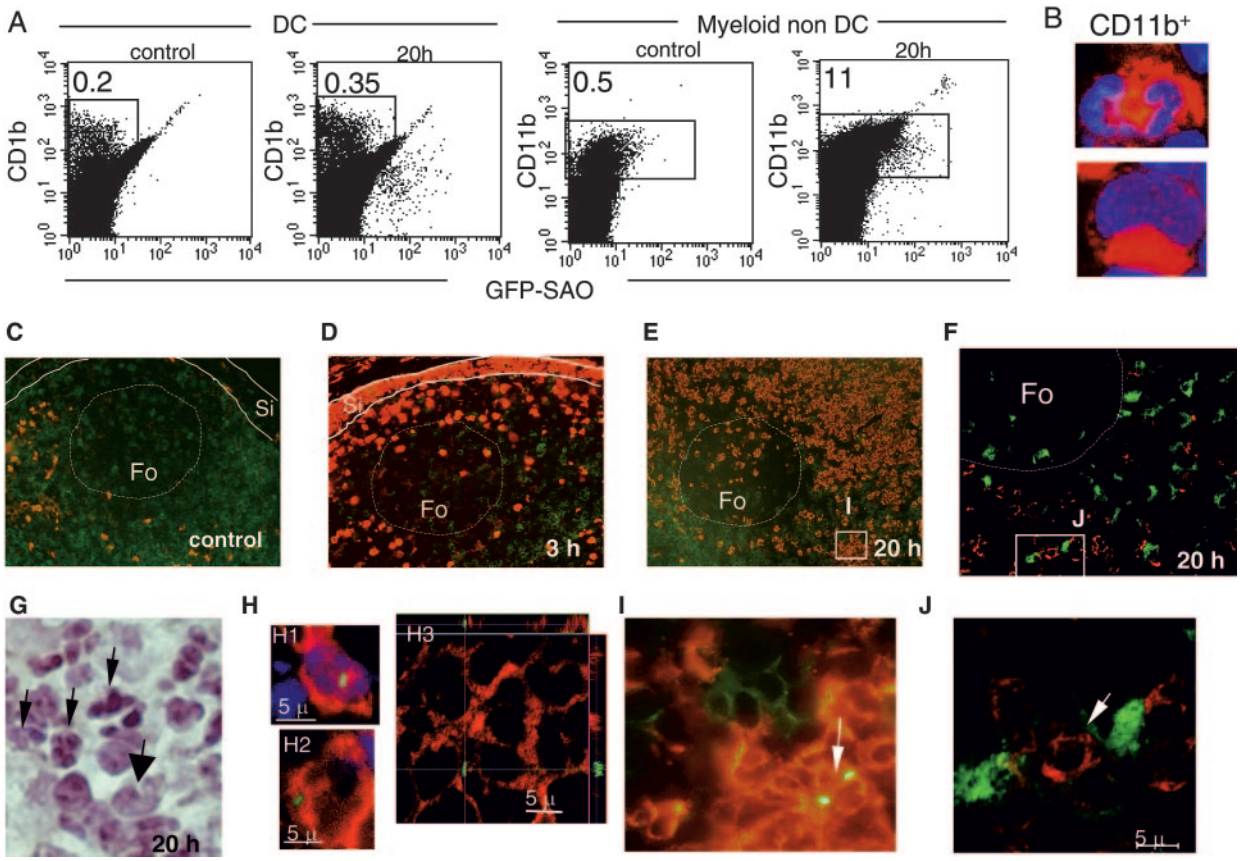

Fig. 1. GFP-SAO induce accumulation of myeloid non-DC in the submaxillary lymph node cortex and are mainly associated with these cells. (A) Lymph node cells were phenotyped with the CD1b and CD11b markers 20 h after injection of GFP-SAO in the oral mucosa [draining (20 h) and contralateral lymph node (control)]. Percent of $CD1b^{pos}$ and $CD11b^{pos}$ cells is indicated (acquisition of 5×10^5 cells). (B) Draining lymph node $CD11b^{pos}$ cells (in red) present a polylobed nucleus (upper) or a horseshoe (lower)-shaped nucleus (DAPI staining in blue), suggesting that they are granulocytes and macrophages, respectively. (C; original, ×20) A subcapsular and perifollicular zone of a control sheep submaxillary node with rare $CD11b^{pos}$ cells (red) and $CD3^{pos}$ T cells (green). The sinus (Si) and follicle (Fo) locations are shown. (D; original, ×20) At 3 h post-GFP-SAO administration in the oral mucosa, the subcapsular area of the draining submaxillary node was filled with $CD11b^{pos}$ cells (red). $CD3^{pos}$ T cells are in green. (E; original, ×20) At 20 h post-administration, $CD11b^{pos}$ cells (red) infiltrated the interfollicular area and were found in the paracortical T cell zone with $CD3^{pos}$ T cells in green. (F; original, ×20, confocal) At 20 h post-administration, $CD11b^{pos}$ cells (in red) were found in the interfollicular and parafollicular areas, forming clusters with DC-$LAMP^{pos}$ cells (in green). (G; original, ×63) At 20 h, an interfollicular zone is visualized by hemalun staining; cells with granulocyte and macrophage morphology are pointed out with fine and large arrows, respectively. (H) Higher magnifications of $CD11b^{pos}$ cells (red) with GFP-SAO are shown: H1 (original, ×100) a granulocyte (fragmented nucleus); H2 (original, ×100) a macrophage (horseshoe nucleus); H3 (confocal, original, ×63 and zoom 5) a bacteria is shown inside a $CD11b^{pos}$ cell. (I; original, ×63) GFP-SAO are seen associated with $CD11b^{pos}$ cells in the T cell zone (a blow-up from E). (J; a blow-up from F) a cluster of DC-$LAMP^{pos}$ cells in green and $CD11b^{pos}$ cell in red is analyzed by confocal; the arrow indicates intimate interactions between cytoplasmic projections of DC and $CD11b^{pos}$ cells. This imaging experiment was done in two sets of three sheep, and results were similar in submaxillary (oral injection) and parotidian (eye-lid injection) lymph nodes. (B–E, G, H1, H2, and I) Obtained with conventional microscopy; (F, H3, J) by confocal microscopy.

(88%; **Fig. 3, A** and **B**). In the cell fraction (Fig. 3A), GFP-SAO was mainly associated with $CD14^{int}$ (32% of the cell-associated SAO) and $CD14^{hi}$ cells (52%) and more rarely with $CD1b^{pos}$ cells (15%). In addition, when lymph cells were cytocentrifuged on a slide (Fig. 3B), GFP-SAO was visualized associated with DC (CD1b staining), granulocytes (CD11b and DAPI staining), and monocytes (CD14 and DAPI staining). At 6 and 20 h after administration, GFP-SAO transport in lymph could still be detected but less frequently and was more confined to the cell fraction (70%) as compared with the 90-min time-period (data not shown). The relative contribution of the different cell subsets in SAO transport appeared similar to their contribution at 90 min, although it was more difficult to evaluate reliably as a result of the rarity of positive events (200 times less frequent at 20 h relative to 90 min). The increased output of myeloid cells was observed during 72 h (data of the kinetic from one sheep are shown; Fig. 3C).

SAO injection induces a lymphatic influx of semi-mature DC

A sorting of the $CD1b^{pos}$ lymph cells by FACS was followed by MGG staining or by DAPI counterstaining and revealed that these cells have a typical morphology of veiled cell (**Fig. 4A**). In addition, the $CD1b^{pos}$ cells corresponded to a distinct population with high FSC and SSC (Fig. 4A). In a previous study, we showed that lymph DC express CD80, CD86, and high levels of CD40 and MHC 2 at their surface [8], indicating that these cells were migrating at a semi-mature state, as suggested by others [23]. Furthermore, we show here that lymph DC already coexpress in intracellular vesicles DC-LAMP and

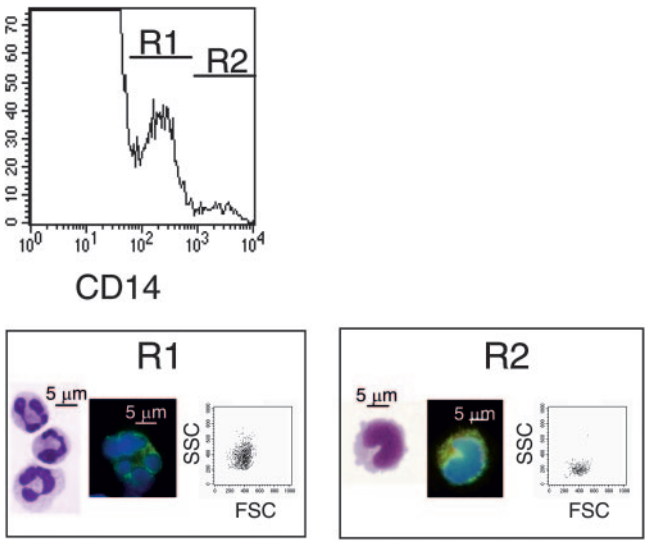

Fig. 2. CD14 level of expression defines lymph granulocytes ($CD14^{int}$) and monocytes ($CD14^{hi}$). Cervical lymph cells were labeled with anti-CD14 (CAM36A) revealed by FITC-GAM. The forward scatter $(FSC)^{hi}$/side-scatter $(SSC)^{hi}$ cells corresponding to DC (see Fig. 4) were excluded by appropriate gating, as these cells have a high autofluorescence that perturbs the analysis. The CD14 staining profile of FSC^{lo} cells reveals two distinct regions, i.e., R1 ($CD14^{int}$) and R2 ($CD14^{hi}$), which were sorted with a FACSCalibur, cytospinned, and stained with MGG or by Alexa Fluor 488-conjugated rabbit anti-FITC and DAPI for nuclear staining. Over 90% of the sorted cells in R1 and R2 gates presented typical morphology of granulocytes and monocytes, respectively.

MHC 2 (Fig. 4B), further confirming their intermediate state of maturation at the migratory stage [24]. After injection of SAO, the recruited DC were analyzed for their surface expression of CD80, CD86, CD40, and MHC 2. No difference of activation marker expression nor surface MHC 2 could be detected on DC at any of the analyzed time-points (90 min, 6 h, 48 h, 24 h, 72 h; Fig. 4C shows the FACS analysis at T0 and T24 h). Finally, the SAO-induced DC were not more potent at inducing MLR (Fig. 4D). This finding indicates that SAO induces an increased output of DC without a detectable sign of enhanced maturation at the lymphatic stage.

SAO injection induces a lymphatic output of monocytes and granulocytes, which presents slightly modified phenotypes compared with its blood counterparts

To determine whether lymph recruitment of monocytes and granulocytes was associated with cell activation and phenotypic changes, these cells were analyzed in three different sheep at several time-points after SAO injection (i.e., 90 min, 6 h, 24 h, 48 h, 72 h) in comparison with blood counterparts. Lymph monocytes and granulocytes expressed higher levels of CD11b than blood monocytes and granulocytes (**Fig. 5**; one representative animal at 24 h). However, CD62L, which is often down-modulated by myeloid cell activation, was not modulated on either cell type (Fig. 5). CD11c nor MHC 2 nor CD86 was up-regulated on lymph monocytes and granulocytes, suggesting that these cells did not acquire a feature of DC-like cells, despite their translocation in lymph. CD40 was found extinguished on lymph monocytes, whereas it was expressed at low levels in blood (Fig. 5A). It is interesting that lymph granulocytes constantly expressed CD80 at all times, whereas blood granulocytes were negative for CD80. Altogether, these data show that lymph monocytes and granulocytes share many phenotypic similarities with their blood counterparts and with a higher level of CD11b on lymph monocytes and granulocytes, lower CD40 on lymph monocytes, and higher expression of CD80 on lymph granulocytes.

DISCUSSION

Our results challenge the linear view of DC being the only and same cell that captures antigen in tissue, migrates, and presents it. They point to three other mechanisms of bacterial antigen transport to nodes in addition to DC, i.e., as free elements in lymph and carriage by monocytes and notably, by granulocytes. They also show that bacteria trigger a lymphatic influx of DC and of myeloid non-DC capable of shuttling the antigen, thus influencing efficiency of antigen delivery in nodes. Finally, myeloid non-DC, including macrophages and granulocytes, were found in the T cell zone and were making intimate interactions with DC. Overall, our data strongly suggest that myeloid non-DC, such as monocytes and granulocytes, link innate to adaptive immunity by migrating with tissue invaders toward lymph node.

Real-time probing of lymphatic traffic allowed visualizing that a large fraction of SAO travels passively in lymph, as reported for soluble antigens [2]. Free SAO could be picked up in the node, possibly in the subcapsular area where monocytes/macrophages, granulocytes, and to a lesser extent, DC initially accumulate rapidly (Fig. 1). The administration volume (50 μl) and the number of injected bacteria (10^9 total, which corresponds to a vaccine dose) may be responsible for the high proportion of free bacteria in lymph. However, free *Salmonella* were also found in lymph after 24 h, further confirming the occurrence of passive transport after the initial overspill.

Semi-mature DC contributed, as expected, to this antigen carriage, although they were much less involved in this process than other phagocytes. Our data indicate DC only account for 15% of bacterial transport by cells in lymph. This finding is in agreement with the observation of Randolph et al. [3], who reported that only 10% of the latex particles found in lymph

TABLE 2. Lymph Cell Influx Induced by SAO

	Collected cells in 90 min ($\times 10^5$ cell)[a]			
Subset	Baseline[b] Sheep 1, 2, 3	SAO[c] Sheep 1, 2, 3	Fold increase[d] Sheep 1, 2, 3	Mean fold increase ± SEM
CD1b	10.5, 7.5, 4.5	22.5, 16.8, 10.1	2.14, 2.2, 2, 2	2.2 ± 0.04
$CD14^{int}$	3.7, 2.5, 9.2	14, 17.5, 33.4	3.8, 7, 3.6	4.8 ± 1.4
$CD14^{hi}$	3.4, 0.9, 2.5	10.8, 11.2, 8.6	3.1, 12.4, 3.4	6.3 ± 4

[a] Lymph output of each subset was calculated based the percentage of the cell subset and the total lymph cell output during 90 min collection periods before[b] and after[c] SAO injection (values for three sheep, respectively). [d] The cell subset fold increase in lymph was calculated for each sheep.

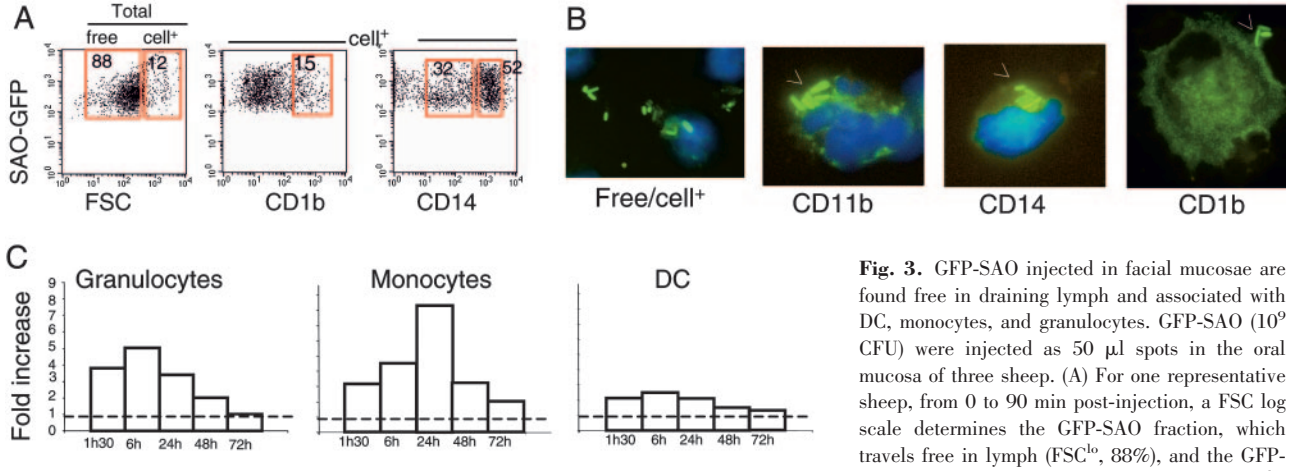

Fig. 3. GFP-SAO injected in facial mucosae are found free in draining lymph and associated with DC, monocytes, and granulocytes. GFP-SAO (10^9 CFU) were injected as 50 µl spots in the oral mucosa of three sheep. (A) For one representative sheep, from 0 to 90 min post-injection, a FSC log scale determines the GFP-SAO fraction, which travels free in lymph (FSC^{lo}, 88%), and the GFP-SAO fraction, which is associated with cells (FSC^{hi}, 12%). The lymph cell fraction positive for SAO was analyzed for the relative contribution of CD1b (15%), $CD14^{int}$ (32%), and $CD14^{hi}$ (52%) cells involved in SAO transport. Similar results were obtained with two other sheep. (B) Free GFP-SAO and cell (CD11b/DAPI-stained)-associated bacteria are shown in the left panel. Cyto-spotted lymph cells were stained for detection of CD11b (MM12A), CD14 (CAM36A), and CD1b (Th97A) followed by FITC-GAM, and for the two latter, nuclei were counterstained in DAPI. A granulocyte ($CD11b^{pos}$, segmented nucleus), monocyte ($CD14^{pos}$, bean-shaped nucleus), and DC ($CD1b^{pos}$) transporting GFP-SAO (indicated with a white arrow) are shown. (C) Recruitment of myeloid cells over time (rate fold increase relative to control) is represented for one sheep. Time-period collections were 0–1 h, 30 min; 1 h, 30 min–6 h; 20–24 h; 44–48 h; and 68–72 h. In two other sheep, a similar pattern of cell recruitment was observed.

node arrived via tissue-derived DC after s.c. injection. In addition, bacterial injection recruited DC to lymph, with an output level reaching twice the basal one's for over 24 h (Fig. 3C). This increased number of DC that reach lymph node may further enhance the efficiency of immune response by increasing the efficiency of naive T cell scanning, thus impacting on T cell priming [25]. Lymph DC at steady state present a semi-mature phenotype. However, administration of SAO did not alter the expression level of MHC 2 and costimulatory molecules at the lymphatic stage, as also reported for intestinal lymph DC after intravenous lipopolysaccharide administration [26]. It is possible that fully activated DC may appear once they gain specific areas of lymph node or only if the bacteria interact directly with the DC.

$CD14^{hi}$ monocytes were also found importantly involved in bacterial transport. This finding is supported by previous reports in mice, showing that particulates (latex) are mainly carried to lymph nodes by blood-derived monocytes [3, 4, 27].

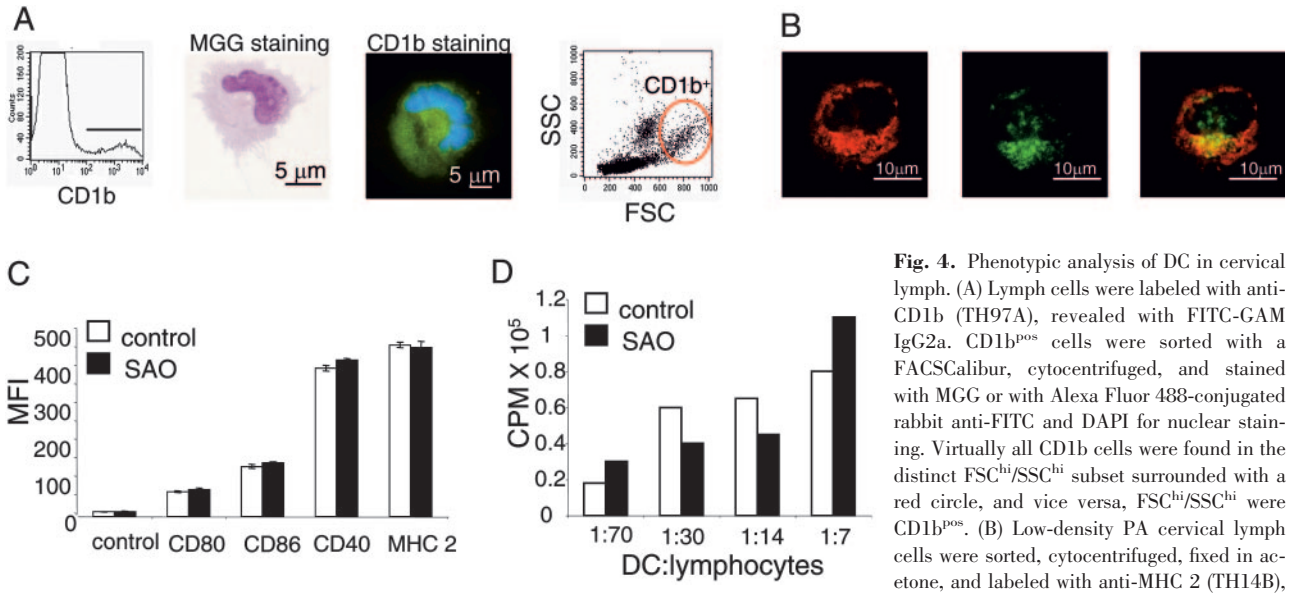

Fig. 4. Phenotypic analysis of DC in cervical lymph. (A) Lymph cells were labeled with anti-CD1b (TH97A), revealed with FITC-GAM IgG2a. $CD1b^{pos}$ cells were sorted with a FACSCalibur, cytocentrifuged, and stained with MGG or with Alexa Fluor 488-conjugated rabbit anti-FITC and DAPI for nuclear staining. Virtually all CD1b cells were found in the distinct FSC^{hi}/SSC^{hi} subset surrounded with a red circle, and vice versa, FSC^{hi}/SSC^{hi} were $CD1b^{pos}$. (B) Low-density PA cervical lymph cells were sorted, cytocentrifuged, fixed in acetone, and labeled with anti-MHC 2 (TH14B), followed by a TRITC-GAM IgG2a, and with the anti-DC-LAMP (104.G4) mAb followed by a FITC-GAM IgG1. Confocal microscopy revealed cytosolic MHC 2 expression, cytosolic DC-LAMP expression, and overlap of the two staining. (C) Lymph cells were collected for 4 h before (control) and for a period between 20 and 24 h after SAO injection (SAO). Cells were stained for CD1b (TH97A, PE-GAM IgG2a) and for the simultaneous detection of CD80 (ILA159), CD86 (ILA190), CD40 (ILA156), MHC 2 (CAT82A), and isotype control revealed by tricolor-GAM IgG1. The geometric mean of fluorescence for the activation marker on CD1b cells of three sheep (mean±SEM) is reported. MFI, Mean fluorescence intensity. (D) $CD1b^{pos}$ cells of one sheep were sorted from lymph collected 4 h before (control) and for a period between 20 and 24 h after SAO injection (SAO), reacted at different ratios with 10^5 allogeneic $CD4^{pos}$ T cells, and tested for [^{3}H]-thymidine incorporation after 96 h culture. CPM, Counts per minute.

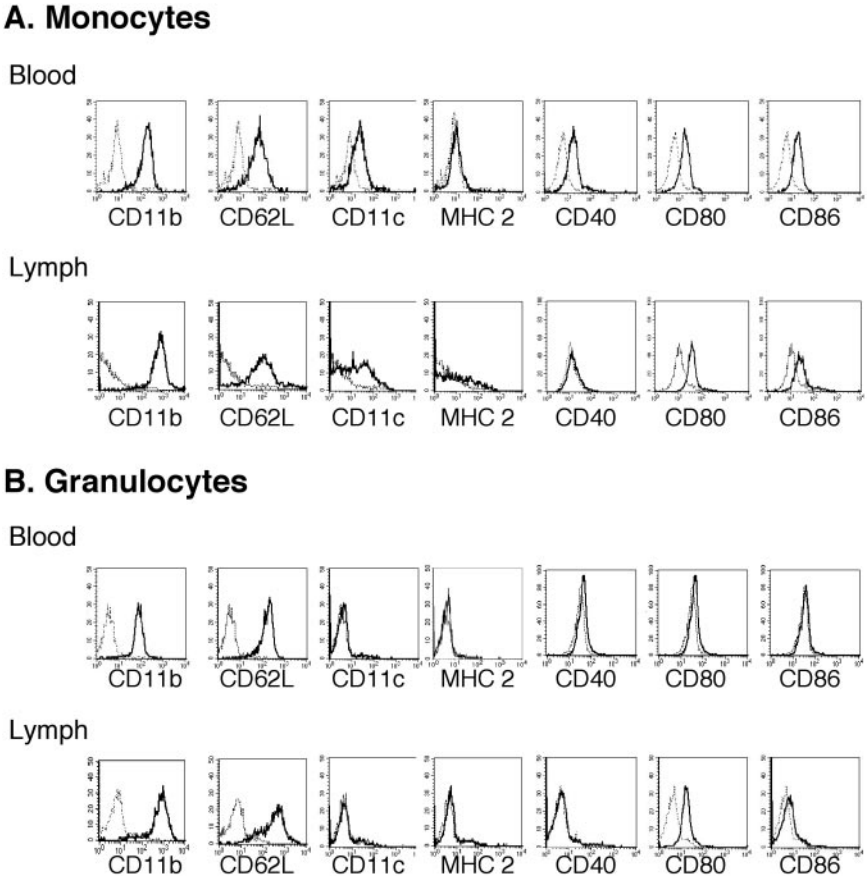

Fig. 5. Phenotypic characterization of blood and lymph monocytes (A) and granulocytes (B). PBMC (for blood monocyte analysis) and PBL (for blood granulocyte analysis) were collected from sheep blood harvested on citrate. Lymph cells were collected between 20 and 24 h post-SAO. Cells were reacted with PE-conjugated anti-CD14 mAb (TUK4, IgG2a) and mAb (IgG1) directed against CD11b (MM12A), CD62L (DU1-29), CD11c (OM1), MHC 2 (CAT82A), CD40 (ILA156), CD80 (ILA159), CD86 (ILA 190), and isotype control revealed with a tricolor anti-GAM IgG1. Monocytes were analyzed by gating on $CD14^{hi}$ FSC^{lo}/SSC^{lo} cells. Granulocytes were analyzed by gating on the $CD14^{int}$ FSC^{lo}/SSC^{hi} cells. Specific staining is shown with thick lines, relative to isotype control with dashed lines. One sheep example is presented. Similar profiles were obtained with two other sheep. The lymph profiles were similar at all times tested before and after SAO administration (90 min, 6 h, 48 h, 72 h).

These monocytes appear to belong to the major circulating subset of monocytes, the inflammatory type [3, 28]. In mice and in human [28], inflammatory monocytes phenotypically correspond to the $CD14^{hi}CD11b^{hi}CD62L^{hi}CD11c^{int}CD80^{lo}CD86^{lo}$ MHC 2^{lo} cells, which we identified in sheep lymph. Although such cells can differentiate in DC-like cells in mice lymph node [3, 28], they still look like bona fide monocytes in lymph, without veiled cell morphology, MHC 2, or CD86 up-regulation. The only difference with classical blood monocytes was a higher level of CD11b and lower level of CD40. The up-regulation of CD11b, also found for lymph granulocytes, can be related to their activation, allowing diapedesis through a vascular wall. However, CD62L was not reduced on lymph monocytes and granulocytes, although myeloid cell activation often leads (but not always) to shedding of this molecule [29].

Salient information provided by direct analysis of lymph resides in the discovery that SAO induces a lymph influx of granulocytes that contributes to SAO transport. Our results confirm a previous study describing an influx of neutrophils in draining lymph nodes after administration of fully virulent and attenuated SAO, but this study did not evaluate the origin of the neutrophils [15]. Until recently, granulocytes were known to reach lymph nodes from blood via high endothelium venules. It is interesting that our data demonstrate, by probing lymph directly, that granulocytes can also gain lymph node with antigens via afferent lymph under inflammatory conditions. In agreement with our finding, a recent report brings evidence that neutrophils shuttle *Mycobacterium bovis* BCG in lymph [7]. Whereas granulocytes were described in lymph at the steady state [30–32] and before SAO injection in our report, it is difficult to know whether their presence at a low level is physiological or a result of the simple presence of the catheter, even weeks after the surgery in healthy sheep and healed surgical scarf. We can speculate that a small basal turnover of granulocyte exists, especially in the lymphatic drainage of the highly exposed mucosae of the head. In any event, we demonstrated that administration of GFP-SAO induced a clear, rapid, and quite sustained (48 h) influx of granulocytes in afferent lymph and in the subcapsular and T cell area of nodes, supporting the occurrence of granulocyte traffic from tissue to nodes under provoked inflammatory conditions. Besides, in accordance with previous knowledge, granulocytes were also recruited from blood in the paracortex, as these cells were also found surrounding lymph node blood endothelium (not shown).

The influx of lymph granulocytes transporting bacteria may have complex effects on the resulting immune response. As granulocytes were found in the paracortex, one can speculate that the granulocyte mission may not be simply to destroy an excess of antigen. Actually, granulocytes can play a role in antigen presentation by regurgitating peptides [33] and can serve for in vivo cross-priming to CD8 T cells [34]. They may also differentiate into antigen-presenting cells [35, 36]. However, in our system, they do not express CD86 or MHC 2 at the lymphatic stage, and they still looked like typical granulocyte in lymph node. Yet, we consistently found that lymph granulocytes expressed CD80, whereas blood granulocytes were $CD80^{neg}$ (Fig. 5). It is interesting that in mice, $CD80^{pos}$ $GR1^{pos}$ cells were identified as immunomodulatory cells in *Candida*

albicans infection, leading to suppression of T helper cell type 1 activation [37]. It is thus possible that the lymphatic influx of $CD80^{pos}$ granulocytes contributes to negatively regulate adaptive immunity to avoid an overwhelming immune reaction. Conversely, in human, activated blood neutrophils trigger antigen presentation by DC via CD11b/DC-SIGN interaction [38].

DC are not the only cells that travel in lymph with captured antigens from tissue; inflammatory monocytes and especially granulocytes are also involved, even to a much higher extent, and should thus be considered as possible important partners in the induction of immune response. Granulocytes may not have received much attention before because of their short lifespan, although recent reports underlined their active role, positive or negative, in immunity. As bacteria-mediated delivery of exogenous antigens become increasingly popular in vaccine strategy, knowledge about the implication of different cells that transport them to decisional lymph node is mandatory to manipulate properly the tuning of immune responses.

ACKNOWLEDGMENTS

This work was supported by institutional grants from the Institut National de la Recherche Agronomique. The authors are grateful to Jean-Pierre Albert, Christian Bourgeois, Franck Gérard, and Isabelle Raoult for their highly efficient technical support in sheep surgery. They thank C. Howard for providing mAb and C. Grüner (Beckman-Coulter) for allowing the testing of the 104.G4 mAb. They also thank Jean-François Alkombre, Joseph Balluais, and Raymond Lavergne for their care to the animals, Phillipe Fontanges (IFR 65, Paris) for confocal microscopy, and Isabelle Dubi for secretarial assistance. The authors thank Pierrette Menanteau and Maggy Grayon for the production of GFP-SAO strains and inocula preparations. They are very grateful to Wayne Hein and Bertrand Schwartz for their critical and constructive reading of the manuscript and Joan Lunney for her support and advice.

REFERENCES

1. Cavanagh, L. L., Von Andrian, U. H. (2002) Travelers in many guises: the origins and destinations of dendritic cells. *Immunol. Cell Biol.* **80,** 448–462.
2. Itano, A. A., McSorley, S. J., Reinhardt, R. L., Ehst, B. D., Ingulli, E., Rudensky, A. Y., Jenkins, M. K. (2003) Distinct dendritic cell populations sequentially present antigen to CD4 T cells and stimulate different aspects of cell-mediated immunity. *Immunity* **19,** 47–57.
3. Randolph, G. J., Inaba, K., Robbiani, D. F., Steinman, R. M., Muller, W. A. (1999) Differentiation of phagocytic monocytes into lymph node dendritic cells in vivo. *Immunity* **11,** 753–761.
4. Rotta, G., Edwards, E. W., Sangaletti, S., Bennett, C., Ronzoni, S., Colombo, M. P., Steinman, R. M., Randolph, G. J., Rescigno, M. (2003) Lipopolysaccharide or whole bacteria block the conversion of inflammatory monocytes into dendritic cells in vivo. *J. Exp. Med.* **198,** 1253–1263.
5. Harmsen, A. G., Mason, M. J., Muggenburg, B. A., Gillett, N. A., Jarpe, M. A., Bice, D. E. (1987) Migration of neutrophils from lung to tracheobronchial lymph node. *J. Leukoc. Biol.* **41,** 95–103.
6. Harmsen, A. G., Muggenburg, B. A., Snipes, M. B., Bice, D. E. (1985) The role of macrophages in particle translocation from lungs to lymph nodes. *Science* **230,** 1277–1280.
7. Abadie, V., Badell, E., Douillard, P., Ensergueix, D., Leenen, P. J., Tanguy, M., Fiette, L., Saeland, S., Gicquel, B., Winter, N. (2005) Neutrophils rapidly migrate via lymphatics after *Mycobacterium bovis* BCG intradermal vaccination and shuttle live bacilli to the draining lymph nodes. *Blood* **106,** 1843–1850.
8. Epardaud, M., Bonneau, M., Payot, F., Cordier, C., Megret, J., Howard, C., Schwartz-Cornil, I. (2004) Enrichment for a CD26hi SIRP-subset in lymph dendritic cells from the upper aero-digestive tract. *J. Leukoc. Biol.* **76,** 553–561.
9. Liu, L., Zhang, M., Jenkins, C., MacPherson, G. G. (1998) Dendritic cell heterogeneity in vivo: two functionally different dendritic cell populations in rat intestinal lymph can be distinguished by CD4 expression. *J. Immunol.* **161,** 1146–1155.
10. Howard, C. J., Sopp, P., Brownlie, J., Kwong, L. S., Parsons, K. R., Taylor, G. (1997) Identification of two distinct populations of dendritic cells in afferent lymph that vary in their ability to stimulate T cells. *J. Immunol.* **159,** 5372–5382.
11. Bujdoso, R., Hopkins, J., Dutia, B. M., Young, P., McConnell, I. (1989) Characterization of sheep afferent lymph dendritic cells and their role in antigen carriage. *J. Exp. Med.* **170,** 1285–1301.
12. Pardon, P., Sanchis, R., Marly, J., Lantier, F., Guilloteau, L., Buzoni-Gatel, D., Oswald, I. P., Pepin, M., Kaeffer, B., Berthon, P. (1990) Experimental ovine salmonellosis (*Salmonella abortusovis*): pathogenesis and vaccination. *Res. Microbiol.* **141,** 945–953.
13. Chevallier, N., Berthelemy, M., Le Rhun, D., Laine, V., Levy, D., Schwartz-Cornil, I. (1998) Bovine leukemia virus-induced lymphocytosis and increased cell survival mainly involve the CD11b+ B-lymphocyte subset in sheep. *J. Virol.* **72,** 4413–4420.
14. Lantier, F., Pardon, P., Marly, J. (1981) Vaccinal properties of *Salmonella abortus* ovis mutants for streptomycin: screening with a murine model. *Infect. Immun.* **34,** 492–497.
15. Fontaine, J. J., Pepin, M., Pardon, P., Marly, J., Parodi, A. L. (1994) Comparative histopathology of draining lymph node after infection with virulent or attenuated strains of *Salmonella abortusovis* in lambs. *Vet. Microbiol.* **39,** 61–69.
16. Valdivia, R. H., Falkow, S. (1996) Bacterial genetics by flow cytometry: rapid isolation of *Salmonella typhimurium* acid-inducible promoters by differential fluorescence induction. *Mol. Microbiol.* **22,** 367–378.
17. Wigley, P., Berchieri Jr., A., Page, K. L., Smith, A. L., Barrow, P. A. (2001) *Salmonella enterica serovar Pullorum* persists in splenic macrophages and in the reproductive tract during persistent, disease-free carriage in chickens. *Infect. Immun.* **69,** 7873–7879.
18. Gupta, V. K., McConnell, I., Dalziel, R. G., Hopkins, J. (1996) Identification of the sheep homologue of the monocyte cell surface molecule—CD14. *Vet. Immunol. Immunopathol.* **51,** 89–99.
19. Gunnes, G., Jorundsson, E., Tverdal, A., Landsverk, T., Press, C. M. (2004) Accumulation of CD25+ CD4+ T-cells in the draining lymph node during the elicitation phase of DNCB-induced contact hypersensitivity in lambs. *Res. Vet. Sci.* **77,** 115–122.
20. Gupta, V. K., McConnell, I., Hopkins, J. (1993) Reactivity of the CD11/CD18 workshop monoclonal antibodies in the sheep. *Vet. Immunol. Immunopathol.* **39,** 93–102.
21. Bassoe, C. F., Smith, I., Sornes, S., Halstensen, A., Lehmann, A. K. (2000) Concurrent measurement of antigen- and antibody-dependent oxidative burst and phagocytosis in monocytes and neutrophils. *Methods* **21,** 203–220.
22. Sabroe, I., Jones, E. C., Usher, L. R., Whyte, M. K., Dower, S. K. (2002) Toll-like receptor (TLR)2 and TLR4 in human peripheral blood granulocytes: a critical role for monocytes in leukocyte lipopolysaccharide responses. *J. Immunol.* **168,** 4701–4710.
23. Lutz, M. B., Schuler, G. (2002) Immature, semi-mature and fully mature dendritic cells: which signals induce tolerance or immunity? *Trends Immunol.* **23,** 445–449.
24. de Saint-Vis, B., Vincent, J., Vandenabeele, S., Vanbervliet, B., Pin, J. J., Ait-Yahia, S., Patel, S., Mattei, M. G., Banchereau, J., Zurawski, S., Davoust, J., Caux, C., Lebecque, S. (1998) A novel lysosome-associated membrane glycoprotein, DC-LAMP, induced upon DC maturation, is transiently expressed in MHC class II compartment. *Immunity* **9,** 325–336.
25. MartIn-Fontecha, A., Sebastiani, S., Hopken, U. E., Uguccioni, M., Lipp, M., Lanzavecchia, A., Sallusto, F. (2003) Regulation of dendritic cell migration to the draining lymph node: impact on T lymphocyte traffic and priming. *J. Exp. Med.* **198,** 615–621.
26. Turnbull, E. L., Yrlid, U., Jenkins, C. D., Macpherson, G. G. (2005) Intestinal dendritic cell subsets: differential effects of systemic TLR4 stimulation on migratory fate and activation in vivo. *J. Immunol.* **174,** 1374–1384.
27. Qu, C., Edwards, E. W., Tacke, F., Angeli, V., Llodra, J., Sanchez-Schmitz, G., Garin, A., Haque, N. S., Peters, W., van Rooijen, N., Sanchez-Torres, C., Bromberg, J., Charo, I. F., Jung, S., Lira, S. A., Randolph, G. J. (2004) Role of CCR8 and other chemokine pathways in

the migration of monocyte-derived dendritic cells to lymph nodes. *J. Exp. Med.* **200,** 1231–1241.
28. Geissmann, F., Jung, S., Littman, D. R. (2003) Blood monocytes consist of two principal subsets with distinct migratory properties. *Immunity* **19,** 71–82.
29. Diez-Fraile, A., Meyer, E., Paape, M. J., Burvenich, C. (2003) Analysis of selective mobilization of L-selectin and Mac-1 reservoirs in bovine neutrophils and eosinophils. *Vet. Res.* **34,** 57–70.
30. Matsuno, K., Ezaki, T., Kudo, S., Uehara, Y. (1996) A life stage of particle-laden rat dendritic cells in vivo: their terminal division, active phagocytosis, and translocation from the liver to the draining lymph. *J. Exp. Med.* **183,** 1865–1878.
31. Persson Waller, K., Colditz, I. G., Lun, S., Ostensson, K. (2003) Cytokines in mammary lymph and milk during endotoxin-induced bovine mastitis. *Res. Vet. Sci.* **74,** 31–36.
32. Pernthaner, A., Cole, S. A., Gatehouse, T., Hein, W. R. (2002) Phenotypic diversity of antigen-presenting cells in ovine-afferent intestinal lymph. *Arch. Med. Res.* **33,** 405–412.
33. Tvinnereim, A. R., Harty, J. T. (2000) CD8(+) T-cell priming against a nonsecreted *Listeria monocytogenes* antigen is independent of the antimicrobial activities of γ interferon. *Infect. Immun.* **68,** 2196–2204.
34. Tvinnereim, A. R., Hamilton, S. E., Harty, J. T. (2004) Neutrophil involvement in cross-priming CD8+ T cell responses to bacterial antigens. *J. Immunol.* **173,** 1994–2002.
35. Radsak, M., Iking-Konert, C., Stegmaier, S., Andrassy, K., Hansch, G. M. (2000) Polymorphonuclear neutrophils as accessory cells for T-cell activation: major histocompatibility complex class II restricted antigen-dependent induction of T-cell proliferation. *Immunology* **101,** 521–530.
36. Sandilands, G. P., Ahmed, Z., Perry, N., Davison, M., Lupton, A., Young, B. (2005) Cross-linking of neutrophil CD11b results in rapid cell surface expression of molecules required for antigen presentation and T-cell activation. *Immunology* **114,** 354–368.
37. Mencacci, A., Montagnoli, C., Bacci, A., Cenci, E., Pitzurra, L., Spreca, A., Kopf, M., Sharpe, A. H., Romani, L. (2002) CD80+Gr-1+ myeloid cells inhibit development of antifungal Th1 immunity in mice with candidiasis. *J. Immunol.* **169,** 3180–3190.
38. van Gisbergen, K. P., Sanchez-Hernandez, M., Geijtenbeek, T. B., van Kooyk, Y. (2005) Neutrophils mediate immune modulation of dendritic cells through glycosylation-dependent interactions between Mac-1 and DC-SIGN. *J. Exp. Med.* **201,** 1281–1292.